Journal of Fluids and Structures (1998) **12,** 3–15

ON THE EXISTENCE OF A CRITICAL SHEAR PARAMETER FOR CELLULAR VORTEX SHEDDING FROM CYLINDERS IN NONUNIFORM FLOW

S. Balasubramanian†, F. L. Haan Jr.*, A. A. Szewczyk* and R. A. Skop†

† *Division of Applied Marine Physics, Rosenstiel School of Marine and Atmospheric Science, University of Miami, Miami, Florida 33149, U.S.A.*

* *Department of Aerospace and Mechanical Engineering, University of Notre Dame, Notre Dame, Indiana 46556, U.S.A.*

(Received 27 November 1996 and in revised form 23 September 1997)

The results of an experimental and numerical investigation into the existence of a critical shear parameter for cellular vortex shedding are presented. The experimental investigation of vortex shedding from a tapered cylinder in a linear shear flow reveals that vortex shedding is cellular, even when the shear in the flow is high. High shear parameters were achieved by orienting the tapered cylinder such that the shear in the flow added to the effect of the taper in the cylinder. Numerical simulations of the high shear experiment using a diffusive Van der Pol oscillator also indicate cellular shedding. The excellent qualitative and quantitative agreement between the numerical simulations and the experimental results validates a unique linear relationship between the shear parameter and a turbulent kinematic viscosity that scales the diffusive axial coupling term in the model.

1. INTRODUCTION

Vortex shedding from bluff bodies in shear flows has been observed to break down into a series of spanwise cells. The frequency of vortex shedding is constant in each cell, but varies from cell to cell. The spanwise variation is a result of the nonuniformity in the approaching flow field. A similar spanwise variation and cell structure has also been observed by placing a tapered cylinder in a uniform flow field. Recently, Balasubramanian & Skop (1996) modelled the experimentally observed cellular shedding patterns from uniform and tapered cylinders in uniform and shear flows by using a diffusively coupled Van der Pol equation. They developed a relationship between p, the nondimensional turbulent kinematic viscosity of the fluid that scales the diffusive term, and a parameter β that characterizes the shear in the flow, such that $p = C\beta$. For details of this effort and use of the Van der Pol equation, we refer the reader to our recent paper (Balasubramanian & Skop 1996).

Balasubramanian & Skop found a discrepancy between the value of C required to simulate the experiments of Woo *et al.* (1981) and all of the other available experimental evidence considered. They found that, while a value of $C = 0{\cdot}0004$ was required to model the data of Woo *et al.*, a value of $C = 0{\cdot}013$ was required for the other experiments. All of the experiments that were considered overlapped in the fundamental parameters that govern the vortex-shedding response from a bluff body; namely, the length-to-diameter

0889–9746/98/010003 + 13 $25.00/fl970122

ratio, Reynolds number, shear parameter, etc., thereby raising a question as to the reason for this discrepancy. The discrepancy could be due to differences in free-stream turbulence or blockage effects, or the amount of fluid withdrawal that was applied to minimize end effects in the experiments of Woo *et al.*; or if one ignores the low-shear data point of Woo *et al.*, it is possible to postulate the existence of a critical shear parameter above which the lower value of C is required.

In an effort to resolve the dual-valued nature of the relationship between the shear in the flow and the turbulent kinematic viscosity, experiments were conducted using a linearly tapered cylinder in a linearly sheared flow, with a shear screen oriented such that the taper in the cylinder augments the shear in the flow to produce high shear parameters. Experimental results provide conclusive evidence that indicates that a cellular structure still persists at higher shear parameters. The nonlinear oscillator model was then used to numerically simulate the vortex-shedding response of the tapered cylinder in the shear flow. Good quantitative agreement with the experimentally determined shedding frequencies and cell patterns was obtained with $C = 0{\cdot}013$, while little agreement was found with $C = 0{\cdot}0004$. This leads us to believe that the results of Woo *et al.* were influenced by certain of their experimental procedures which are discussed in our conclusions. The present paper details the results of the experiments and the numerical simulations.

2. EXPERIMENTAL SETUP

The experiments were conducted in a sub-sonic wind tunnel located in the Hessert Center for Aerospace Research at the University of Notre Dame. The tunnel is of the in-draft type and has an inlet contraction ratio of 20·6 : 1. The speed capability of the tunnel ranges from 3 to 30 m/s. The experiments reported here were conducted at a mean velocity of 11·5 m/s. A linear shear profile could be produced by placing an S-shaped screen upstream of the test section. The test section is 183 cm long and has a 61 cm × 61 cm cross-section. A tapered solid aluminium cylinder was mounted horizontally and spanned the tunnel. The diameter of the cylinder varied from 2·54 cm on one end to 5·08 cm on the other. The taper ratio of the cylinder, $R_r = L/(D_L - D_0)$ was 23·8. End-plates that were 29·21 cm long and 15·25 cm wide, constructed from 0·64 cm thick Plexiglas, were used to alleviate end effects. The length of the cylinder between the end-plates was 41·28 cm. We introduce here an axial coordinate system, denoted by z, with its origin at the end-plate at the small diameter end. The diameter at $z = 0$ is given by $D_0 = 3{\cdot}016$ cm and the diameter at $z = L = 41{\cdot}28$ cm is $D_L = 4{\cdot}76$ cm and corresponds to the location of the other end-plate. Figure 1 shows a schematic of the experimental setup.

Hot-wire measurements were made using a Dantec 55P01 single-wire probe. The probe had a tungsten wire sensor of 5 μm diameter and operated in a constant-temperature mode. The analog signal from the hot wire was analysed wth a TSI (IFA100) anemometer. The probe was mounted on a digitally controlled three-degree-of-freedom traverse, with an overall probe positioning accuracy of 1·0 mm in the streamwise and spanwise directions and an accuracy of 0·1 mm in the vertical direction. Power spectral density measurements of the near wake were recorded at 15 spanwise locations along the cylinder. The hot-wire probe was positioned at a distance of 3·3 cm above the centreline of the cylinder and at a distance of 10·16 cm behind the cylinder axis. This corresponds to a location of $(0{\cdot}65D^*, 2D^*)$, where D^* corresponds to the largest diameter (5·08 cm) of the tapered cylinder.

The vortex shedding from the tapered cylinder was studied under three flow conditions: a uniform flow; a linearly sheared flow for which the maximum flow velocity corresponded

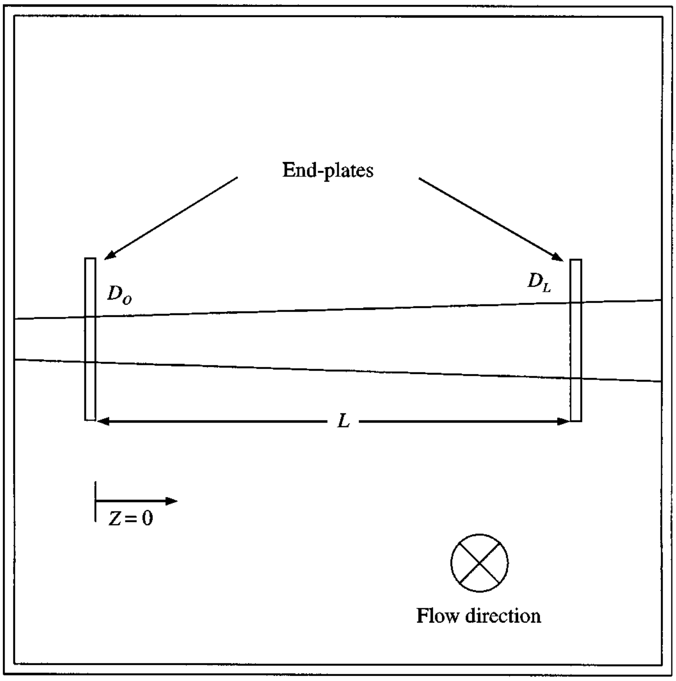

Figure 1. Schematic of the cross-section of the wind tunnel showing the arrangement of the tapered cylinder and the end-plates.

to the large-diameter end of the cylinder; and a linearly sheared flow for which the maximum flow velocity corresponded to the small-diameter end of the cylinder. The first two experiments were conducted to ascertain the reproducibility of results previously reported by Anderson & Szewczyk (1995).

Velocity profiles were recorded for the uniform flow test case and for the two shear flow scenarios. To accomplish this, a Pitot tube was attached to the traverse mechanism and velocities were recorded at various spanwise positions. The uniform flow profile had an average velocity of 11·35 m/s. For the shear flow profile in which the maximum velocity corresponded to the large diameter end of the cylinder, the velocity varied between 11·2 m/s at the small-diameter end to 14·2 m/s at the large-diameter end. The flow gradient was computed to be $-8{\cdot}37\,\mathrm{s}^{-1}$. For the reversed shear flow profile, the velocity at the large-diameter end was 8·35 m/s and increased to 12·4 m/s at the small-diameter end. The flow gradient was computed to be $8{\cdot}33\,\mathrm{s}^{-1}$. The uniform and shear flow profiles and the linear regressions for the flow gradients are shown in Figure 2.

The shear in the flow, for experiments on vortex shedding, is parametrized by a non-dimensional shear parameter β, defined by

$$\beta = \frac{D_{\mathrm{ref}}}{\omega_{s,\max}} \left| \frac{\mathrm{d}\omega_s}{\mathrm{d}z} \right|. \tag{1}$$

Here, ω_s is the intrinsic vortex-shedding frequency, $\omega_{s,\max}$ is the maximum value of ω_s along the cylinder, and D_{ref} is the diameter of the cylinder at the axial location at which $\omega_{s,\max}$

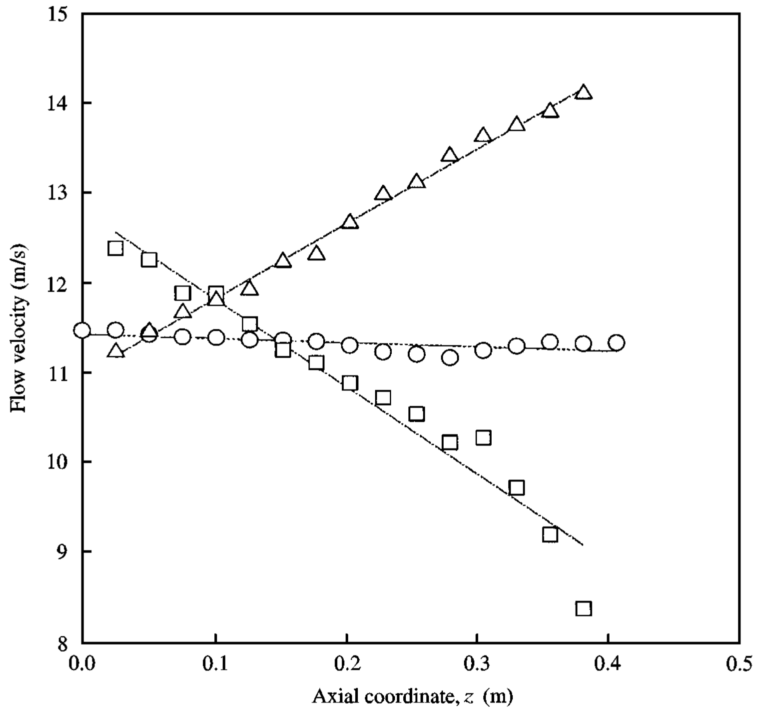

Figure 2. Uniform and shear flow profiles. Open circles (○) represent the uniform flow profile. Open squares (□) represent the shear flow for which the maximum flow velocity corresponded to the large-diameter end of the cylinder. Open triangles (△) represent the shear flow profile in which the maximum flow velocity occurred at the small-diameter end of the cylinder. Solid lines represents linear regressions to the data.

occurs. The intrinsic vortex-shedding frequency is given by

$$\omega_s = 2\pi S \frac{V}{D}, \tag{2}$$

where S is the Strouhal number, V is the local velocity and D is the local diameter. For our experiments, the Reynolds number based on cylinder diameter was on the order of 36 000 and the Strouhal number can be assumed to be a constant with a value of $S = 0{\cdot}21$. The diameter at any point along the cylinder is given by

$$D = D_0 + S_2 z, \tag{3}$$

where $S_2 = 1/R_T$. Similarly, the velocity is given by

$$V = V_0 + S_1 z, \tag{4}$$

where S_1 is the velocity gradient and V_0 is the velocity at $z = 0$, both obtained from linear regressions to the measured velocity data. Combining equations (1)–(4), the shear parameter is calculated as

$$\beta = \frac{2\pi S D_{\text{ref}}}{\omega_{s,\max}} \frac{|S_1 D_0 - S_2 V_0|}{(D_0 + S_2 z)^2}. \tag{5}$$

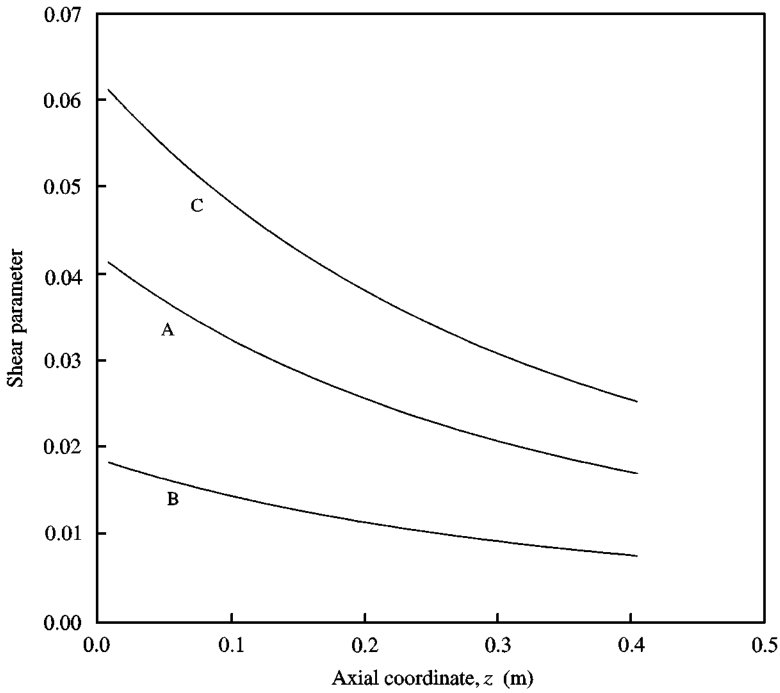

Figure 3. Variation of the shear parameter along the cylinder, Curve A corresponds to a tapered cylinder in uniform flow; curve B to the tapered cylinder in an adverse shear flow; and curve C to the tapered cylinder in an aiding shear flow.

The variation of the shear parameter along the cylinder for our experiments is shown in Figure 3. For all three cases $\omega_{s,\max}$ was at $z = 0$. The curve labelled "A" represents the variation of β for the tapered cylinder in uniform flow. The curve labelled "B" corresponds to the experiment in which the shear screen was oriented such that it opposed the effect of the taper in the cylinder, thus resulting in very low shear parameters. Curve "C" corresponds to the experiment in which the shear in the flow added to the taper in the cylinder to create very high shear parameters. The values of β along curve "C" range from approximately 0·03–0·06 and encompass the higher shear values in the experiments of Woo *et al.* (1981).

3. EXPERIMENTAL RESULTS

The power spectral densities at the 15 spanwise measurement locations for the three cases studied are shown in Figures 4–6. Cellular vortex shedding was observed in all three cases. As seen in Figure 4, when the tapered cylinder is placed in a uniform flow, the frequency of vortex shedding varies from about 51 Hz at the large-diameter end to about 78 Hz at the small-diameter end.

When a linear shear is introduced in the oncoming flow such that it offsets the influence of the taper of the cylinder, a partial cancellation of the spanwise variation of the vortex-shedding frequency is observed. The shedding frequency varies only by 6 Hz over the length of the cylinder as seen in Figure 5, since the net nonuniformity in the flow is reduced. The

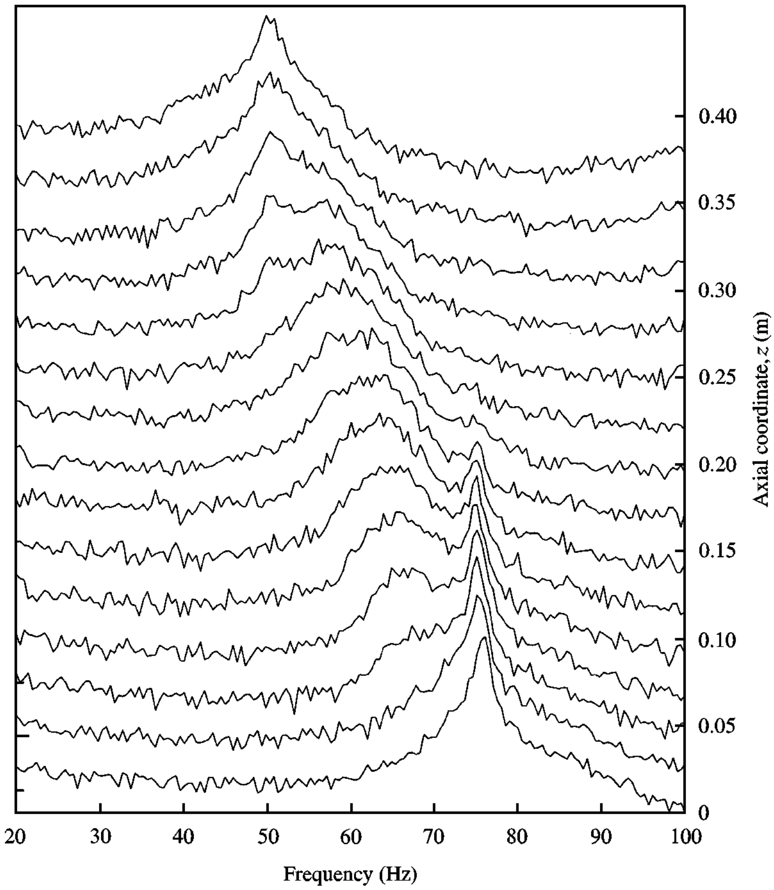

Figure 4. Experimentally observed vortex-shedding pattern from the tapered cylinder in a uniform flow.

qualitative agreement between Figure 5 and the power spectral density plot as obtained by Anderson (1995) [see Figure 12 in Balasubramanian & Skop (1996)] is excellent. In Anderson's experiments, the flow gradient was $6{\cdot}2\,s^{-1}$ with a maximum flow speed of 12·9 m/s, as opposed to $8{\cdot}37\,s^{-1}$ and 14·17 m/s in our experiments.

When the shear screen is oriented such that shear in the flow adds to the effect of the taper in the cylinder, a greater variation of the shedding frequency over the length of the cylinder is observed. The vortex-shedding frequency varies from 36 Hz at the large-diameter end to 79 Hz at the small-diameter end of the cylinder. As seen in Figure 6, distinct cells at 79 and 36 Hz at the ends are evident. The cell structure between the two end cells is not very marked and seems to exhibit a broad-band nature. This can be attributed to a change in the shear layer structure, which results from the addition of the shear in the oncoming flow and the taper of the cylinder.

The results of these experiments indicate that there exists no breakdown in the cellular nature of vortex shedding when the shear parameter is high. High levels of shear results in broad-band shedding frequencies away from the ends, but distinct end-cells are still present.

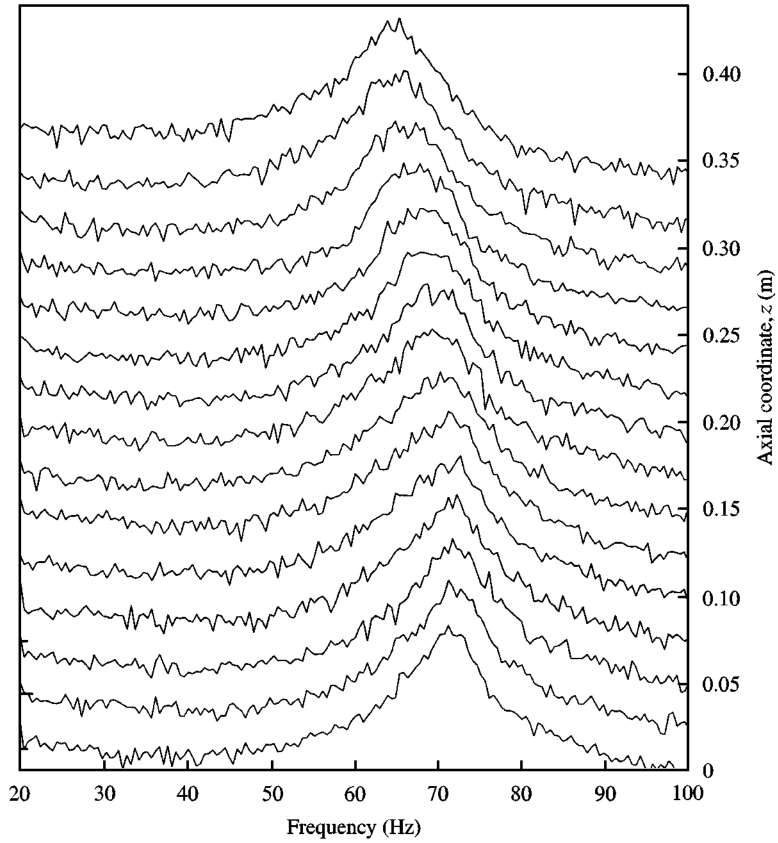

Figure 5. Experimentally observed vortex-shedding response from the tapered cylinder in an adverse shear flow.

4. NUMERICAL SIMULATION

The diffusive Van der Pol oscillator has been shown to be a successful model for the vortex-shedding response of uniform and tapered cylinders in uniform and shear flows (Balasubramanian & Skop 1996). The model equation in nondimensional form is

$$\frac{\partial^2 u}{\partial \tau^2} + \varepsilon \Omega_s (u^2 - 1) \frac{\partial u}{\mathrm{d}\tau} + \Omega_c^2 u - p \left(\frac{L}{D_{\mathrm{ref}}} \right)^2 \frac{\partial^3 u}{\partial \xi^2 \partial \tau} = 0, \tag{6}$$

where $u(\xi. \tau)$ is defined as a dimensionless fluid quantity such as a component of the velocity, $\tau = \omega_{s,\max} t$ is the nondimensional time and $\xi = z/D_{\mathrm{ref}}$ is the dimensionless axial coordinate. The nondimensional vortex-shedding frequency along the cylinder is $\Omega_s(\xi) = \omega_s/\omega_{s,\max}$. The dimensionless diffusion coefficient that scales the diffusive term is given by $p = v_t/(L^2 \omega_{s,\max})$, where v_t has been interpreted by Skop & Balasubramanian (1995b) to be a turbulent kinematic viscosity. The scaling parameter ε has been taken by Skop & Balasubramanian (1995a) to be $\varepsilon = 0{\cdot}2$.

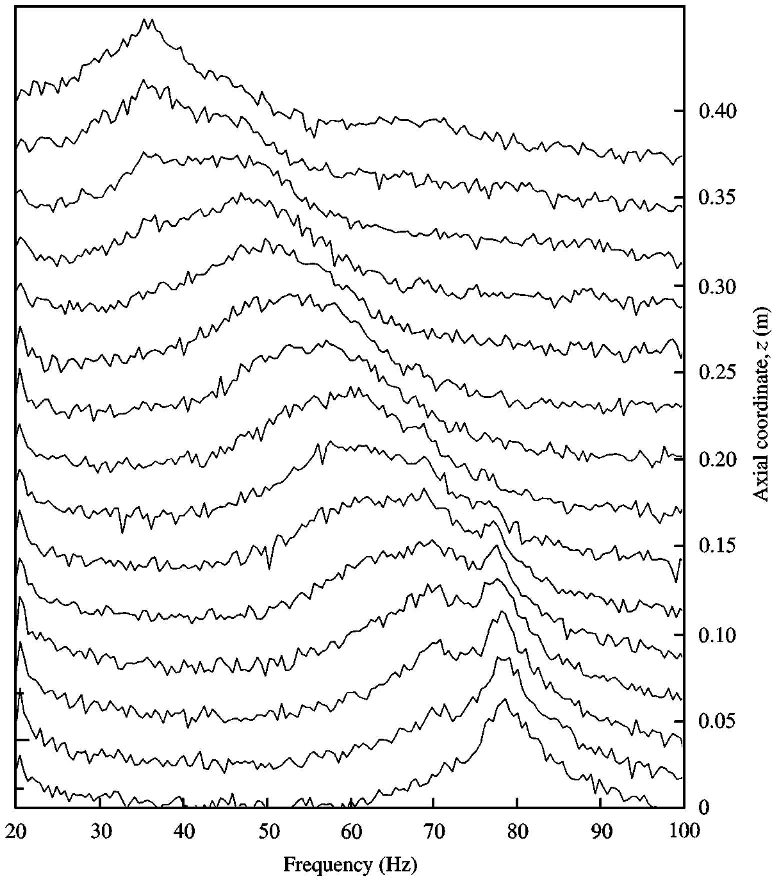

Figure 6. Experimentally observed vortex-shedding response of the tapered cylinder in an aiding shear flow.

Skop & Balasubramanian (1995b) matched the experimentally observed cellular vortex-shedding patterns of uniform cylinders in linear shear flows by varying the value of p and developed a linear relationship between p and the shear parameter β given by $p = C\beta$, where $C = 0{\cdot}0004$ for the experiments of Woo *et al.* and $C = 0{\cdot}013$ for all other experimental evidence considered. Later, Balasubramanian & Skop (1996) successfully used the linear relationship with $C = 0{\cdot}013$ to model the vortex-shedding response of tapered cylinders and cones in uniform and shear flows.

The diffusive Van der Pol equation was discretized and integrated numerically using a fourth-order Runge–Kutta technique with parameters corresponding to those of the experiments described in the previous section. The time histories of the near-wake fluid dynamic quantity $u(\xi, \tau)$ were then transformed into frequency domain using a Fast Fourier Transform. The details of these numerical techniques remain the same as in Balasubramanian & Skop (1996).

The numerical simulation of the spanwise variation of the vortex-shedding frequency of the tapered cylinder in uniform flow is shown in Figure 7. The quantitative agreement in the shedding frequencies between the experiment (Figure 4) and the numerical simulation is

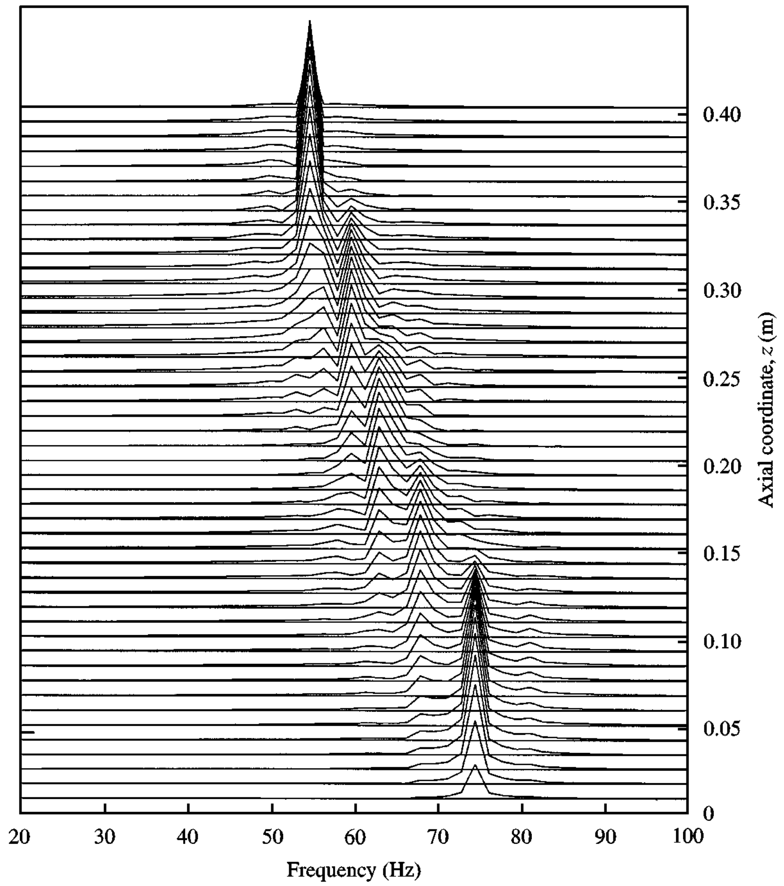

Figure 7. Numerically simulated vortex-shedding response of the tapered cylinder in a uniform flow — cf. Figure 4.

good. Two strong end cells at 76 and 52 Hz are evident, with the model displaying three constant-frequency cells between the end-cells that are not quite so evident in the experimental results. The amplitudes of the spectral peaks for the simulations are on a linear scale as opposed to the log scale used for the experiments.

The results of the numerical simulation of the tapered cylinder in the adverse shear flow are shown in Figure 8. As expected, the variation in the shedding frequency along the span of the cylinder is reduced. The frequencies range from about 66 Hz at the large-diameter end to about 72 Hz at the small-diameter end and compare very well with the experimental results as seen in Figure 5.

For the case of a tapered cylinder in an aiding shear flow, the results of the numerical simulation, as seen in Figure 9, display two distinct end-cells and a broad response between the two end-cells that is very similar to the experimentally observed vortex-shedding pattern. The end-cell at the small-diameter end in the numerical simulation occurs at 78 Hz, while the other end-cell at the large-diameter end occurs at 43 Hz. The corresponding end-cell in the experimental results occurs at 36 Hz. The reason for the discrepancy arises from the fact that the numerical simulations were done using the linear regressions to the

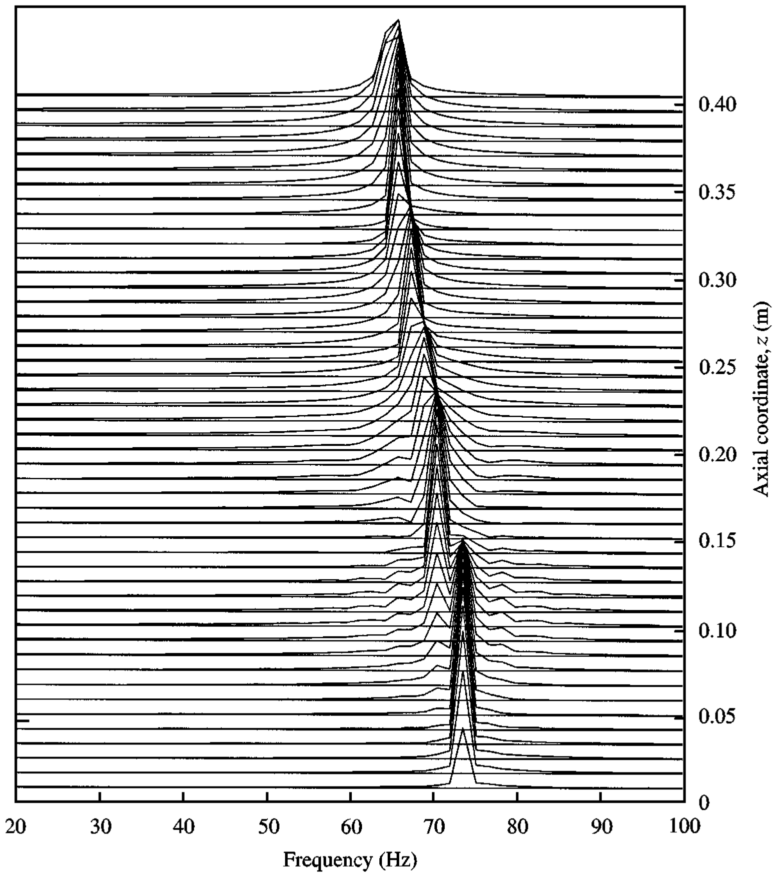

Figure 8. Numerically simulated vortex-shedding response of the tapered cylinder in an adverse shear flow — cf. Figure 5.

measured velocity data. The linear regression yields a value of 9·45 m/s for the velocity at the large-diameter end, while the measured velocity at the location is 8·34 m/s, as seen from Figure 2. This difference in velocity corresponds to a difference of 7 Hz in the vortex-shedding frequency.

5. ANALYSIS AND CONCLUSIONS

The results of the experiments on the vortex-shedding response from a tapered cylinder in an aiding shear flow and the numerical simulation for the same flow configuration indicate that there is no breakdown in the cellular nature of vortex shedding. The diffusive Van der Pol oscillator, with a linear relationship between the dimensionless diffusion coefficient p and the shear parameter β, given by $p = 0{\cdot}013\beta$, has been shown to be capable of modelling the vortex-shedding response of a tapered cylinder in an aiding shear flow. The results of the diffusively coupled oscillator with $C = 0{\cdot}0004$ for the tapered cylinder in aiding shear flow are shown in Figure 10. The model results do not display the experimentally observed broad-band nature away from the ends. In fact, there is no discernible cellular structure when a value of $C = 0{\cdot}0004$ is used.

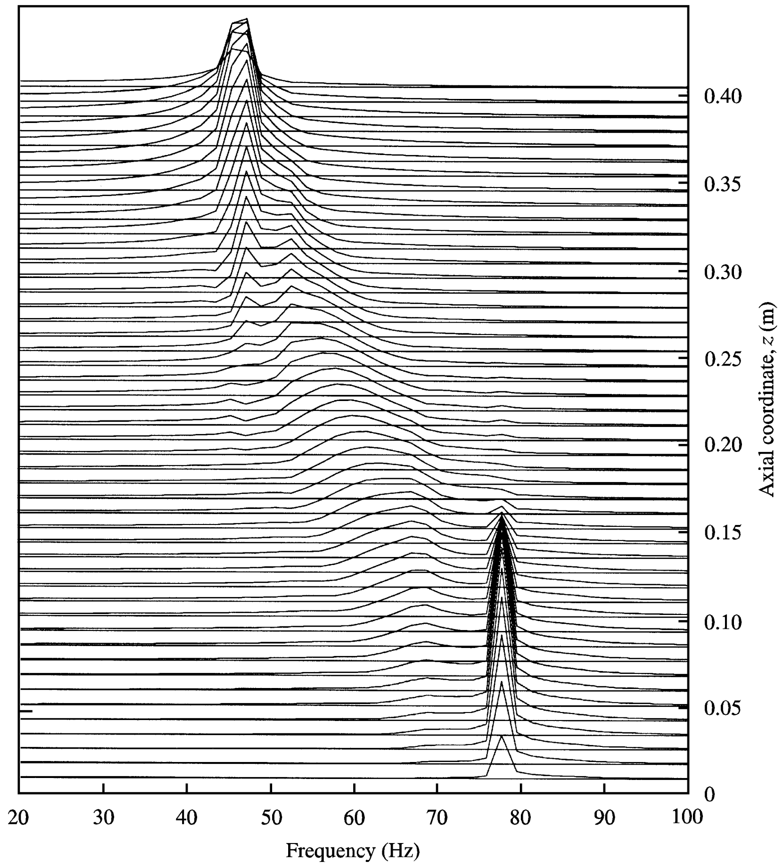

Figure 9. Numerically simulated vortex-shedding pattern of the tapered cylinder in an aiding shear flow with $C = 0{\cdot}013$ — cf. Figure 6.

The results of Woo *et al.* (1981) on the vortex-shedding response of a uniform cable in a linear shear flow display a weak cellular structure compared to other available experimental evidence. In a later discussion of their experiments, Woo *et al.* (1989) note that " . . . it was decided to leave some gaps between the cylinder and the end plates. In addition to this, at the top [sic, high speed] end of the cylinder on the lee side, an air pump was used to reduce the local pressure at the "dead end" by continuous removal of air." The purpose of these procedures was to avoid build-up of an adverse pressure gradient near the ends of the cylinder. Meanwhile, the other available experiments used simple end-plates or very high L/D ratio cylinders to reduce tunnel-wall boundary layer effects.

In conclusion, both the experimental evidence and the results of the numerical simulations indicate that there exists no breakdown in the cellular nature of vortex shedding when the shear parameter is high. The quantitative and qualitative agreement between the numerical simulation and experimental results for a tapered cylinder in aiding shear flow is excellent when the linear relationship between p and β is given by $p = 0{\cdot}013\beta$. The need for a lower value of C ($C = 0{\cdot}0004$) to model the data of Woo *et al.* (1981) can be attributed to the end conditions employed in their wind tunnel. These conditions apparently lead to the weak cellular structure observed in their experiments.

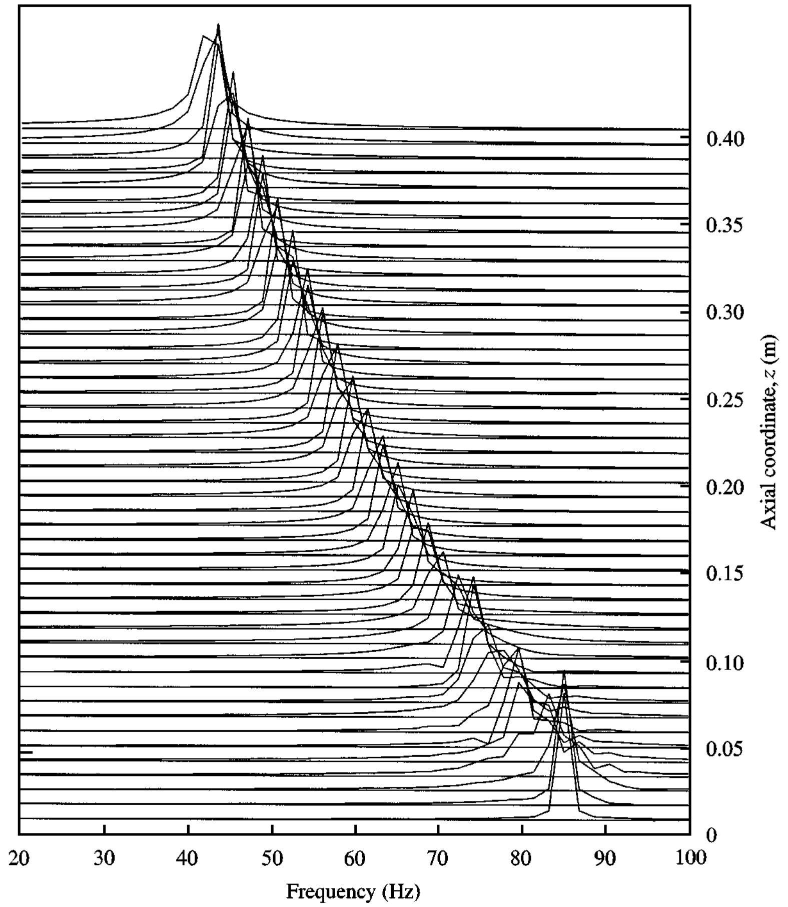

Figure 10. Numerically simulated vortex shedding response for a tapered cylinder in an aiding shear flow with $C = 0{\cdot}0004$.

ACKNOWLEDGMENTS

The authors gratefully acknowledge the support of the U.S. Office of Naval Research under Grant Numbers N00014-93-1-0438, N00014-96-1-0756 and N00014-90-1-4083 for the work reported in this paper.

References

Alberéde, P. & Monkewitz, P. A. 1992 A model for the formation of oblique shedding and "Chevron" patterns in cylinder wakes. *Physics of Fluids* A **4**, 744–756.

Anderson, E. A. 1994 Effects of taper and splitter plates on the near wake characteristics of a circular cylinder in uniform and shear flow. Ph.D. dissertation, University of Notre Dame, IN 46556, U.S.A.

Anderson, E. A. & Szewczyk, A. A. 1995 Vortex shedding from straight and tapered cylinders in shear flows. *Proceedings Sixth International Conference on Flow Induced Vibration*, London, U.K., pp. 61–71. Rotterdam: Balkema.

BALASUBRAMANIAN, S. & SKOP, R. A. 1996 A nonlinear oscillator model for vortex shedding from cylinders and cones in uniform and shear flows. *Journal of Fluids and Structures* **10**, 197–214.

SKOP, R. A. & BALASUBRAMANIAN, S. 1995a A nonlinear oscillator model for vortex shedding from a forced cylinder in a shear flow. Part I: Uniform flow and model parameters. *International Journal of Offshore and Polar Engineering* **5**, 251–255.

SKOP, R. A. & BALASUBRAMANIAN, S. 1995b A nonlinear oscillator model for vortex shedding from a forced cylinder in a shear flow. Part 1: Shear flow and axial diffusion. *International Journal of Offshore and Polar Engineering* **5**, 256–260.

WOO, H. G. C., CERMAK, J. E. & PETERKA, J. A. 1981 Experiments on vortex shedding from stationary and oscillating cables in a linear shear flow. Report on CSU Project 5-32453, Colorado State University, Fort Collins, CO, U.S.A.

WOO, H. G. C., CERMAK, J. E. & PETERKA, J. A. 1989 Secondary flows and vortex formation around a circular cylinder in constant shear flow. *Journal of Fluid Mechanics* **204**, 523–542.